OPEN ACCESS Freely available online

AFM Applied Functional Materials

ISSN 2737-5323
Volume 2, Issue 3
https://www.iikii.com.sg/journal/AFM
Applied Functional Materials

Article

Nanostructuring Polyaniline Using Non-Substituted Imidazolium-Based Ionic liquid as Polymerization Medium Enabling Faster Supercapacitor Operation

Fatima Al-Zohbi [1,2], Fouad Ghamouss [1,3,*], Bruno Schmaltz [1], Mohamed Abarbri [1], Khalil Cherry [2], Mohamad fadel Tabcheh [4] and François Tran-Van [1,*]

[1] Laboratoire de Physico-Chimie des Matériaux et des Electrolytes Pour l'Energie (EA 6299), University of Tours , Parc de Grandmont 37200 Tours, France; alzohbi-fatima@hotmail.com (F. A-Z.) bruno.schmaltz@univ-tours.fr (B.S.); mohamed.abarbri@univ-tours.fr (M.A.)
[2] Laboratoire Matériaux, Catalyse, Environnement et Méthodes Analytiques (MCEMA) Campus Universitaire de Hadath, Liban; khalil.cherry@ul.edu.lb (K.C)
[3] Materials Science and Nano-engineering, Mohammed VI Polytechnic University, Lot 660 Hay Moulay Rachid, Ben Guerir, Morocco
[4] Laboratoire de chimie appliquée, Faculté des sciences III, Universite Libanaise, Kobbeh - Tripoli – Liban ; mtabcheh@ul.edu.lb (M.T)
***** Correspondence: fouad.ghamouss@um6p.ma (F.G.), francois.tran@univ-tours.fr Tel.: +33 2 47 36 69 23 (F. T-V.)

Received: Jun 29, 2022; **Accepted:** Jul 29, 2022; **Published:** Sep 30, 2022

Abstract: Non-substituted imidazolium-based protic ionic liquid, namely imidazolium hydrogen sulfate [Imi][HSO_4], has been investigated as a polymerization medium for PANI (designated as PANI/PIL). The resulting material was then investigated as electrode materials for supercapacitors. [Imi][HSO_4] was prepared via a one-step acid-base reaction, and its structure was confirmed by ^{1}H NMR. [Imi][HSO_4] displayed full miscibility with water owing to the charge density distribution of its ions. Furthermore, the binary mixture [Imi][HSO_4]/water is highly acid (e.g. pH ~ 0.1 for [Imi][HSO_4]/water in a weight ratio of 70/30). As the polymerization medium for PANI/PIL, [Imi][HSO_4] plays the role of a soft template agent and induces nanostructured PANI formation with fibrillar morphology (as shown by SEM images) without affecting the typical structure of PANI (as confirmed by FT-IR analysis). Furthermore, PANI/PIL was obtained in emeraldine salt form without any undesirable byproduct. Moreover, the electrical conductivity was seven times superior to that of the conventional PANI (i.e. PANI/HCl) when measured by the four-probe technique of PANI/PIL (~ 21.8 S/cm). This improvement in the PANI/PIL's electrical conductivity of as well as the fibrillar morphology of PANI/PIL positively influences its electrochemical performances and highlights the suitability of [Imi][HSO_4] as a polymerization medium for PANI material.

Keywords: Polyaniline, Protic ionic liquids, Polymerization medium, Supercapacitors

1. Introduction

Polyaniline (PANI) is investigated as a material for electrodes for electrochemical supercapacitors in many research works [1–12]. PANI is an inexpensive conducting polymer with organic semiconductors properties and a large surface area. It stores electrochemical energy through a fast reversible redox process involving the catch/release of electrolyte counterion from the polymer [13–16]. The performance of PANI electrodes in electrochemistry strongly correlates with the PANI morphology. The electrolyte counterion diffusion of the polymer is the best in the case of PANI with nanostructured homogeneous morphology [12]. PANI nanowires, for example, with small diameters decrease the distance of the charge transport of the PANI materials that facilitate electrolyte penetration of anions into the inner layer of PANI, and therefore, are used as an electrode material [17].

Recent studies have shown that ionic liquids as a polymerization medium for PANI can control its morphology [17–29]. Indeed, ionic liquids act as a soft template agent for PANI and control its chains during the polymerization process without altering their chemical structure [19–21]. As summarized in a recent review [12], disubstituted ionic liquids based on imidazolium are the most used ionic liquids for PANI since they interact with PANI through non-covalent interactions and induce homogeneous nucleation during the polymerization process. Monosubstituted imidazolium-based ionic liquid has also been studied as a polymerization medium for PANI [29].

Replacing substituted imidazolium (Di or monosubstituted) with non-substituted imidazolium cation-based ionic liquids saves time and money as a multi-step reaction is required to prepare the former while the latter is synthesized through one-step acid-base

reaction. Therefore, the purpose of this study is to show the effectiveness of ionic liquids that are not substituted and are based on imidazolium as a polymerization medium for PANI.

2. Material and Method

2.1. Material

Aniline was distilled before use under reduced pressure. Sulfuric acid (95-98%, Alfa Aesar), imidazole (Sigma Aldrich, ≥ 99.5%), ammonium persulfate $(NH_4)_2S_2O_8$ (98%, Alfa Aesar), hydrochloric acid (57%, Alfa Aesar), polytetrafluoroethylene (60 wt% dispersion in H_2O, Aldrich), carbon black (Timcal, super C65), and activated carbon (Norit, Super DLC-50) were all utilized as supplied. Water was obtained with a Milli-Q 18 purifier.

2.2. Synthesis of [Imi][HSO$_4$]

Imidazolium hydrogen sulfate [Imi][HSO_4] was synthesized by an equimolar acid-base reaction by using the previously described procedure to prepare pyrrolidinium hydrogen sulfate [Pyrr][HSO_4] [27,30]. Briefly, the reaction flask (i.e. a round-bottomed flask with three necks) was iced in a bath and connected to a thermometer, a dropping funnel, and a reflux condenser. Sulfuric acid (43 g, 0.44 mol) was added slowly with the dropping funnel into the flask containing the saturated aqueous solution of imidazole (30 g1, 0.44 mol). The reaction was processed under vigorous stirring at a temperature below 20˚C to avoid the formation of undesirable products since the reaction is exothermic. After finishing the addition of acid, the final solution was stirred for 30 min at 20˚C. Then, the mixture was kept overnight at room temperature under stirring. The product was dried for a day under a vacuum. The collected [Imi][HSO_4] was a dark brown solid with a melting point of 61˚C at room temperature. The molecular formula of [Imi][HSO_4] is $C_3H_5N_2.HSO_4$ and its molecular weight is 166.2 g/mol.

2.3.PANI synthesis

PANI/PIL was synthesized by typical oxidative polymerization of PANI. Briefly, 58.9 g of [Imi][HSO_4] was added to anilinium hydrogen sulfate solution (3 g in 18 mL water) under stirring at 5˚C. The solution of $(NH_4)_2S_2O_8$ (4.56 g in 10 mL of water), cooled to 5˚C, was slowly added to the anilinium solution. The oxidant $(NH_4)_2S_2O_8$ to aniline mole ratio was 1.25/1, and [Imi][HSO_4] to water weight ratio was 70/30 in the final mixture. The mixture was stirred for 24 h at 5˚C. A solid product was collected after filtration and washed in water until a neutral pH. The obtained green powder, designated as PANI/PIL, was then dried at 60˚C for 12h under a vacuum. PANI (PANI/HCl) was prepared by using a conventional method for comparison. It was synthesized by mixing aniline with $(NH_4)_2S_2O_8$ in HCl at 5˚C as described in previous articles [27,31].

2.4. Characterizations

^{1}H spectrum was recorded with the Varian Unity Inova 300 MHz at room temperature. $(CH_3)_4Si$ (TMS, 0 ppm) was the internal standard. The attenuated total reflection infrared (ATR-IR) spectrum was obtained by using a Perkin Elmer (spectrum one model) for the PANI. Scanning electron microscopic (SEM) images were taken by a Zeiss ultra plus field emission (Carl Zeiss Microscopy GmbH, Jena, Germany). This study was performed with PANI powders deposited on standard SEM aluminum studs and metalized platinum (2–4 nm). Thermogravimetric analysis (TGA) was carried out from 25 to 450˚C at a rate of heating at 10˚C/min in a nitrogen environment using the Perkin Elmer model simultaneous thermal analyzer STA 6000. Elemental analysis (C, H, O, S, and N) was conducted using Flash EA 1112 Thermo Finnigan piloted by Eager 300 software. The electrical conductivity of PANI pellets was measured at room temperature with a Keithley 6220 current source and Keithley 2182 A nanovoltmetre using a four-probe technique. Each pellet's thickness was 1200–1300 µm and composed of 200 mg of PANI powders.

The structure of each cluster was adjusted by using Turbomole 7.0 [32,33]. Before visualizing with TmoleX (version 4.1.1), structures were adjusted to a convergence criterion of 10^{-8} Hartree in the gas phase by using the Resolution of Identity (RI) approximation and DFT calculations [34,35]. Turbomole 7.0 and B3LYP function are used with the def-TZVP basis set [36–38].

2.5. Preparation of electrodes and electrochemical characterizations

Electrochemical measurement for each PANI sample was performed at room temperature with two different cell configurations (i.e. symmetric two-electrode cell configuration and three-electrode cell configuration) and H_2SO_4 1 mol/L as electrolyte. These measurements were recorded by the EC Lab V10.32 interface on a versatile multichannel potentiostat (Biologic S.A). For the configuration of the three-electrode cell, the working electrode was made by loading about 1.5 mg/cm^2 of a paste composed of three components on a stainless steel mesh to obtain carbon black (32 wt%), active material PANI (60 wt%), and polytetrafluoroethylene PTFE (8 wt%). The paste was produced following the procedure in Ref. [27]. The three previously mentioned components were introduced in a mortar, and then, ground with a pestle. Afterward, a minimal needed amount of ethanol was added to the powder mixture and stirred with a spatula. The resulting paste was then spread thin on the surface of the glass to get rid of the volatile solvent (i.e. ethanol). The counter electrode was produced by pressing on a stainless steel mesh with a paste (7 mg) containing PTFE (10 wt%), carbon black (20 wt%), and activated carbon (70 wt%) under a pressure of 10 tons. The reference electrode was a saturated calomel electrode. For the symmetric configuration cell with two-electrode, Teflon Swagelok-type system was used. The electrodes were created by loading the paste (3 mg) that was used for the three-electrode cell configuration on a stainless steel mesh (0.8 cm in diameter). The two electrodes were separated with a porous Whatman® membrane (90 mm in pore diameter) immersed in H_2SO_4 1 mol/L.

3. Results and Discussion

The first part of this section details the synthesis and structural characterization of [Imi][HSO_4], while the second one presents the adequacy of [Imi][HSO_4] as a polymerization medium for PANI.

3.1. Part I: Ionic liquid: Imidazolium hydrogen sulfate [Imi][HSO_4]

[Imi][HSO_4] was produced through an equimolar acid-base reaction, and its formation was confirmed by ^{1}H NMR analysis and recorded in deuterated dimethyl sulfoxide DMSO at room temperature (20°C). Figure 1 presents the ^{1}H NMR spectra of [Imi][HSO_4] as well as its starting material (i.e. Imidazole). It was observed that the chemical shift of peaks attributed to the hydrogen (H_1 et H_2) on the carbon atoms of imidazole was increased after the formation of imidazolium. The chemical shift was increased from 7.68 ppm (H_1) and 7.03 ppm (H_2) for imidazole to 8.9 ppm (H_1) and 7.63 ppm (H_2 and $H_{2'}$) in the case of imidazolium. Another ^{1}H NMR spectra showed that the split signal of H_2 was changed from singlet for imidazole to doublet for imidazolium, indicating that the electronic environment of H_2 and H_2' were no longer similar due to the formation of cationic specie (i.e. Imidazolium).

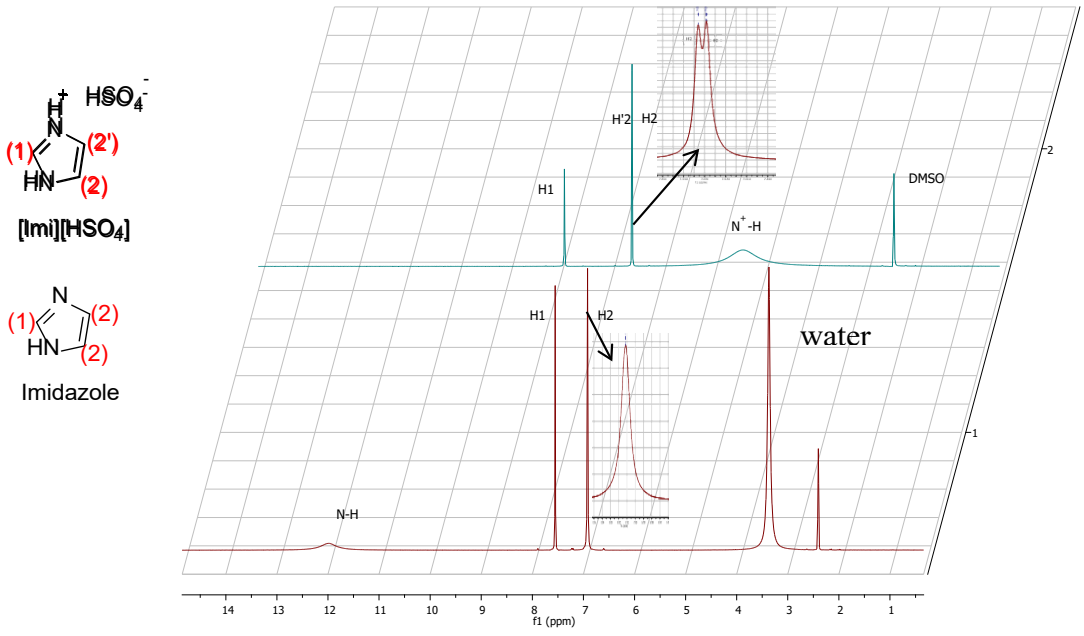

Fig. 1. ^{1}H NMR spectra of [Imi][HSO_4] (red spectrum) and Imidazole (green spectrum) in deuterated DMSO.

[Imi][HSO_4] is highly miscible with water owing to the ionic liquid's protic nature and the charge distribution of its ions. Figure 2(a) shows the 3D molecular surface polarity distributions of imidazolium (Imi^+), hydrogen sulfate (HSO_4^-), and water molecules. For clarity, the mapped surface charge distribution is also shown. For HSO_4^-, the region of positive polarization charge (red region) and that of negative polarization charge (the dark blue surface) were displayed on its total surface, revealing that HSO_4^- strongly interacted with water molecules. Moving to imidazolium (Imi^+), it was clear that the charge (or the blue color) was delocalized between its nitrogens. The delocalized polarization charge on almost the whole surface of HSO_4^- and the important part of Imi^+ reflected relatively weak Coulombic HSO_4^-- Imi^+ interactions. This ionic liquid which was dissociated easily with water at all proportions generates a rich ionic medium that interacts with aniline and therefore acts as a template controlling the structure and the morphology of the resulting PANI material. Thus, to synthesize the PANI, we used the mixture of [Imi][HSO_4]/water in a weight ratio of 70/30 as a compromise between ionic liquid concentration and the viscosity of the mixture. Figure 2(b) illustrates the evolution of the viscosity of the selected binary mixture of [Imi][HSO_4]/water by temperature. The viscosity considerably depended on the temperature. It decreased from 16.5 mPa.s at 5°C to 6.8 mPa.s at 35°C. It was concluded that the [Imi][HSO_4]/water mixture was relatively viscous at the typical polymerization temperature (i.e. 5°C) of aniline. The relatively high viscosity of the selected polymerization medium was related to controlling the speed of nucleation during polymerization.

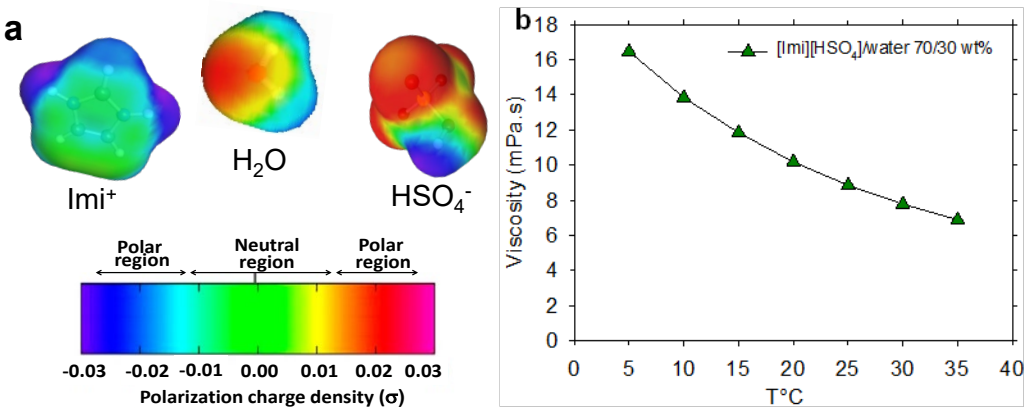

Fig. 2. (**a**) 3D molecular surface charge distributions and surface polarization of imidazolium (Imi^+), hydrogen sulfate (HSO_4^-) and water and (**b**) viscosity values as a function of temperature for [Imi][HSO_4]/water (70/30 wt%).

3.2. Part II: Synthesis, characterization, and morphology of PANI (PANI/PIL vs. PANI/HCl)

PANI/PIL was successfully synthesized via oxidative polymerization in the [Imi][HSO_4]/water mixture under vigorous stirring. For comparison, the conventional PANI (i.e. PANI/HCl) was also produced. PANI/HCl and PANI/PIL were obtained in emeraldine salt form and viewed by ATR-IR. The Emeraldine base form of the obtained PANI/HCl and PANI/PIL was also prepared to study the backbone structure of PANI. An appropriate amount of PANI/PIL or PANI/HCl in emeraldine salt form was dispersed in ammonium hydroxide 1 mol/L in the same manner as described in Ref. [39]. The solution color was switched from green to blue, revealing that the basic emeraldine form of both PANI was obtained. It was filtered and rinsed with water to make pH neutral, and then dried at 60°C under a vacuum. ATR-IR spectra were investigated for the emeraldine salt form of PANI/PIL and PANI/HCl as well as of PANI in the basic emeraldine form of PANI-EB/PIL and PANI-EB/HCl (Fig. 3). As for PANI base form (Fig. 3(a)), the ATR-IR spectra of PANI-EB/HCl and PANI-EB/PIL were superimposed, indicating that their backbone structures were similar. The band of absorption observed at 1493 and 1588 cm^{-1} is associated with the stretched benzene rings (N-B-N) and quinone rings (N=Q=N), respectively [40,41]. These two bands indicate the amine and imine in the polymer. The peak at 1304 cm^{-1} was ascribed to aromatic C-N stretching indicating the secondary aromatic amine group [40,41]. The band at 1151 cm^{-1} was attributed to the in-plane deformation of C–H [40]. The peak at 823 cm^{-1} was correlated to the bending vibration of C-H of benzene rings out-of-plane, indicating that the aromatic rings of PANI are para-disubstituted [40,42,43]. Moving to the AT-IR spectra of PANI in salt form (Fig. 3(b)), the position of all absorption bands was shifted to a lower wavenumber as compared with those of the PANI base form. The red shift was due to the charge delocalization of a conjugated structure [44]. Furthermore, a band of 1286 cm^{-1} appeared and was ascribed to the stretching of C-$N^{+\cdot}$ [45]. Most of the characteristic IR bands of PANI/PIL were moved to lower wavenumber as compared with those of PANI/HCl. This shift was linked to the degree of protonation, or more accurately, to the doping level. The gap between the doping level of PANI/PIL and PANI/HCl was confirmed by thermogravimetric and elementary analysis.

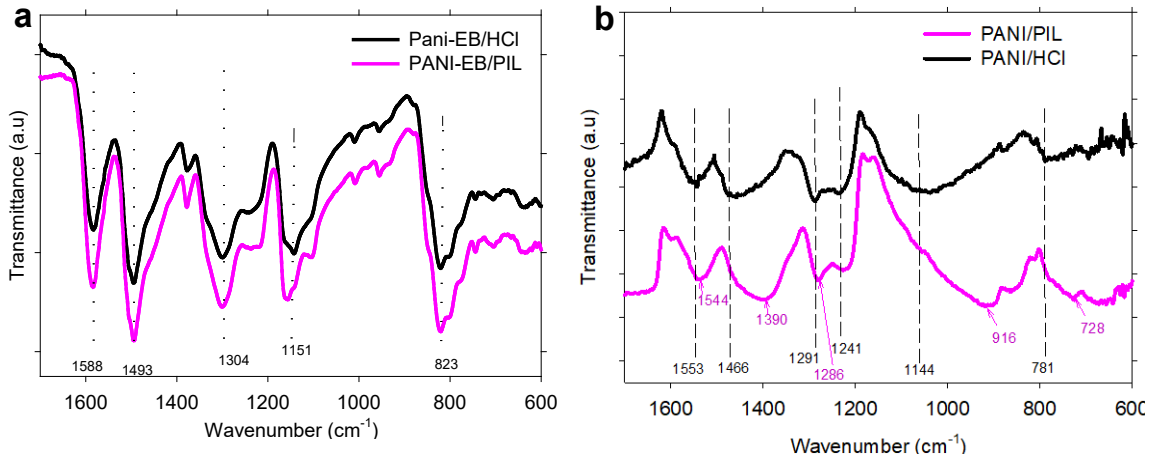

Fig. 3. ATR-IR spectra of (**a**) PANI-EB/HCl and PANI-EB/PIL and (**b**) PANI/PIL and PANI/HCl.

The PANI powder's morphology was obtained by SEM. The SEM images are presented in Fig. 4. The PANI/HCl exhibited an inhomogeneous and agglomerated morphology (Fig. 4(a)), which is consistent with its morphology reported in Refs. [19,46]. However, PANI/PIL displayed a fibrillar morphology (Fig. 4(b)) that was different from the typical granular morphology of PANI doped with sulfuric acid [31,47–49]. The formation of fibrillar morphology of PANI/PIL induced by [Imi][HSO_4] was due to the effect of [Imi][HSO_4] on the polymerization rate. Indeed, during the preparation of PANI/PIL, the dark green color was observed approximately half an hour after all the oxidant agents were added into anilinium solution in [Imi][HSO_4]/water, while this color immediately appeared in the case of PANI/HCl. The delay of the apparition of green color during polymerization of PANI means that the reaction rate was slowed down and nucleation of aniline was affected [29].

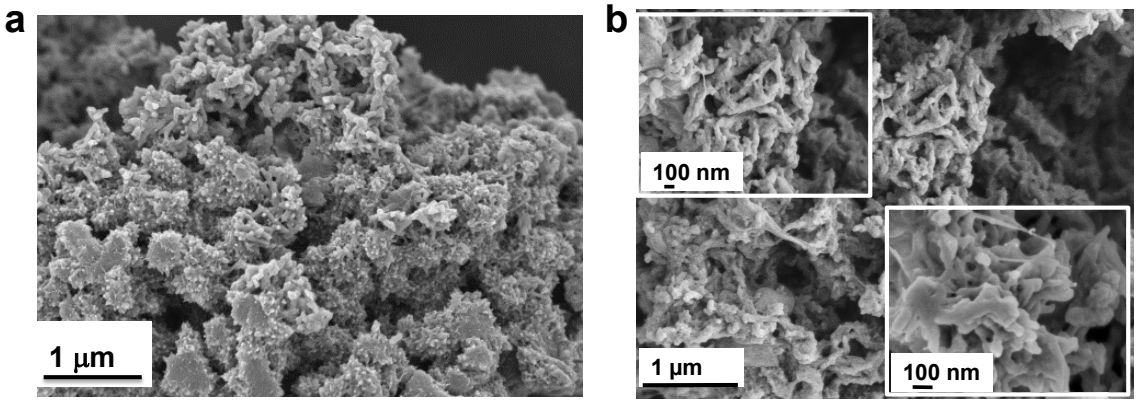

Fig. 4. SEM images of (**a**) PANI/HCl and (**b**) PANI/PIL.

The thermal stability of PANI/HCl and PANI/PIL was studied by using thermogravimetric analysis (TGA). The result is illustrated in Fig. 5. TGA thermograms present three stages of thermal decomposition as typically observed for PANI [50,51]. The first step was water evaporation at 25–100˚C. The water loss was much less for PANI/PIL (2 %) than for PANI/HCl (8 %). In the second step, weight loss occurred because of the loss of the dopant. The dopant loss began at 197˚C for PANI/PIL and PANI/HCl, while the dopant weight loss was substantially higher for PANI/PIL (22.9%) than for PANI/HCl (11.3%). In the third step, weight loss happened because of the decomposition and degradation of the polymer backbone.

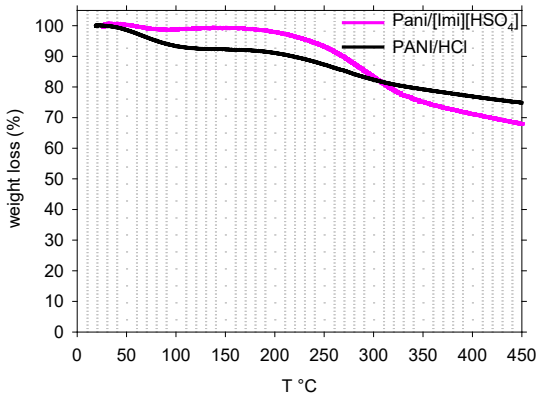

Fig. 5. TGA thermograms of PANI/PIL and PANI/HCl.

The electrical conductivity of PANI/HCl and PANI/PIL was analyzed by the four-point probe method, and the result was summarized in Table 1. The PANI/PIL's electrical conductivity (21.8 S/cm) was seven times higher than that of PANI/HCl (3 S/cm). Moreover, the electrical conductivity of PANI/HCl was consistent with the result of Ref. [52]. The PANI's electrical conductivity depends on the dopant type or doping level of PANI, the pH of the polymerization medium [53–56], and the inter-layer spacing between PANI chains [10,57,58].

The level of the doping of the PANI/HCl and PANI/PIL was estimated via the atomic ratio of S/N as only imine nitrogen atoms are protonated [59]. The element composition of PANI/HCl and PANI/PIL is summarized in Table 1. As for PANI/PIL, the S/N atomic ratio (ca. 0.35) is higher than that of PANI/HCl (ca. 0.15). Furthermore, PANI/HCl is doped with the sulfate group of oxidant agent as well as by chloride ion [60,61], while PANI/PIL is doped with sulfate group derivative from either the anilinium salt [60] or the polymerization medium of [Imi][HSO_4]. Although PANI/PIL and PANI/HCl do not have the same dopant type nor the same doping level, the improvement of the electrical conductivity of PANI/PIL does not affect the dopant type or doping level on account of the results [31].

The electrical conductivity and the S/N atomic ratio of PANI/PIL were compared to those of PANI/[Pyrr][HSO_4] [31] (Table 1). The S/N atomic ratio of PANI/PIL was almost similar to that of PANI/[Pyrr][HSO_4] while the PANI/PIL's electrical conductivity was 12 times higher than that of PANI/[Pyrr][HSO_4]. Since PANI/PIL and PANI/[Pyrr][HSO_4] were doped with the same dopant type and exhibited almost similar doping levels but displayed a different electrical conductivity, was assumed that the relatively high PANI/PIL's electrical conductivity was not related to its dopant type or doping level. Regarding the pH of the polymerization medium, the electrical conductivity of PANI increased along with the increment of protons concentration of the polymerization medium [53]. The pH of the [Imi][HSO_4]/water mixture and [Pyrr][HSO_4]/water (70/30 wt%, pH~0.34) was almost similar. Thus, pH may not be the reason for improving the electrical conductivity of PANI/PIL.

Concerning the arrangement of PANI chains, the synthesis conditions of PANI/PIL and PANI/[Pyrr][HSO_4] were similar except for the polymerization medium type. These two ionic liquids (i.e. imidazolium hydrogen sulfate [Imi][HSO_4] and pyrrolidinium hydrogen sulfate [Pyrr][HSO_4]) interacted differently with PANI. Based on the possible interactions between PANI and disubstituted imidazolium-based ionic liquids [12], [Imi][HSO_4] is thought to interact with PANI, not only via hydrogen bonding interactions but also through π-π interactions. The latter is not possible between [Pyrr][HSO_4] and PANI. Owing to these non-covalent interactions [29,58], the ionic liquid acted as a cross-linked agent and reduced the inter-layer spacing of PANI chains. As the main difference between PANI/PIL and PANI/[Pyrr][HSO_4] was the interactions between PANI and the polymerization medium, these interactions are the reason for the improvement in the electrical conductivity of PANI/PIL.

Table 1. Element composition and electrical conductivity values of PANI/HCl, PANI/PIL and PANI samples reported in our previous work [31]

sample	percentage (%)					atomic ratio	□□(S/cm)	reference
	C	H	N	S	O	S/N		
PANI/HCl	55.6	4.7	11.0	3.7	-	0.15	3	this work
PANI/PIL	47.9	4.5	11.4	9.2	23.2	0.35	21.8	this work
PANI/[Pyrr][HSO_4]	51.1	4.6	10.2	7.1	-	0.3	1.18	[31]

The electrochemical performances of PANI/HCl and PANI/PIL were measured in a three-electrode system configuration by cyclic voltammetry in H_2SO_4 1 mol/L. Figure 6 shows the CV curves of each PANI from -0.4 to 0.6 V vs. SCE at a scan rate of 5 mV/s. On both CV curves, a redox couple is seen and located at almost the same potential. This redox couple is associated with the redox transformation of PANI between the Leucoemeraldine (i.e. semiconducting state) and Emeraldine form (i.e. conducting state) [62].

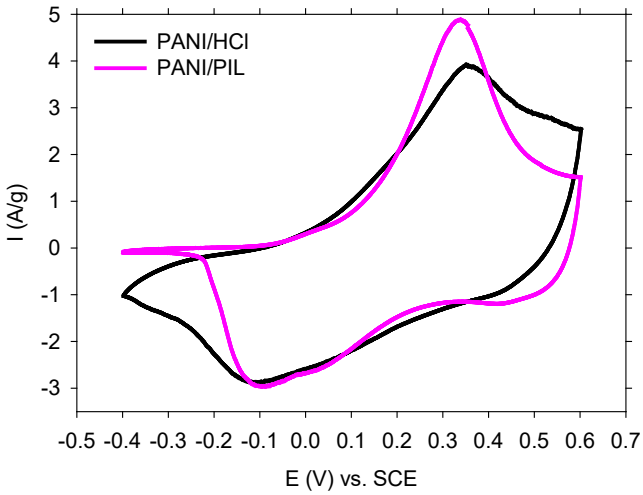

Fig. 6. CV curves of PANI/HCl and PANI/PIL in H_2SO_4 1 mol/L at 5 mV/s recorded using a three-electrode configuration system.

The pseudocapacitive and storage performances of PANI were then studied in a symmetric two-electrode configuration. Figures 7(a) and (b) present the CV curves of PANI/PIL, PANI/HCl, and PANI/[Pyrr][HSO_4] in the voltage range between 0 and 0.55 V at 100 and 15 mV/s, respectively. All the CV curves have a quasi-rectangular shape that confirms the pseudocapacitive behavior of the investigated PANI materials [63]. However, a slight deviation of the CV curve shape from an ideal rectangular shape was more pronounced for PANI/HC due to the lower PANI/HCl electrical conductivity. However, the CV curve shape was closer to the rectangle for PANI/PIL which indicates less polarization resistance when reversing the voltage scan. This difference between the CV curve shape of the investigated PANI affected the dissimilarity of their morphology [17,19,64] or the big gap in the electrical conductivity. Therefore, the CV curves' shape showed that the capacitance performance was better for PANI/PIL as the CV curve for ideal supercapacitors is typically a perfect rectangle [65]. On the other side, a couple of redox peaks were also displayed in the CV curves at a low scan rate (Fig. 7(b)), revealing the faradaic transformation of PANI [63]. This couple was located at the same voltage for all the investigated PANI, which means the same redox reactions occur for all the tested materials.

The specific capacitance was determined based on the discharge curves and the mass of active materials by using the following equation.

$$C = \frac{\int Idt}{mx\,\Delta\,V} \tag{1}$$

In the equation, C is the specific capacitance of the active materials of both electrodes (F/g), I is the constant discharge current (mA), dt is the discharge time (s), ΔV is the voltage difference in discharge (V), and m is the total mass of the active material onto both electrodes (mg). The capacitance was multiplied by 4 to obtain the specific capacitance per electrode mass. The corresponding specific capacitance at various scan rates for PANI/PIL and PANI/HCl is illustrated in Fig. 7(c). The specific capacitance of PANI reduces with increasing the scan rate [63]. When the scan rate increases from 15 to 100 mV/s, the specific capacitance drops from 263, 239, and 193 to 164, 184, and 171 F/g for PANI/HCl, PANI/[Pyrr][HSO_4], and PANI/PIL, respectively. Figure 7(d) presents the specific capacitance retention as a function of the scan rate. When the scan rate increased from 15 to 100 mV/s, the decrease in specific capacitance for PANI/PIL (11%) was much lower than for PANI/[Pyrr][HSO_4] (24%) and PANI/HCl (38%). The sharp decrease in the specific capacitance of PANI/[Pyrr][HSO_4] and PANI/HCl as a function of the scan rate is interpreted by a more favorable and faster diffusion of the electrolyte in the bulk material. In other words, the ionic diffusion path is highly related to the scan rate for PANI/[Pyrr][HSO_4] and PANI/HCl.

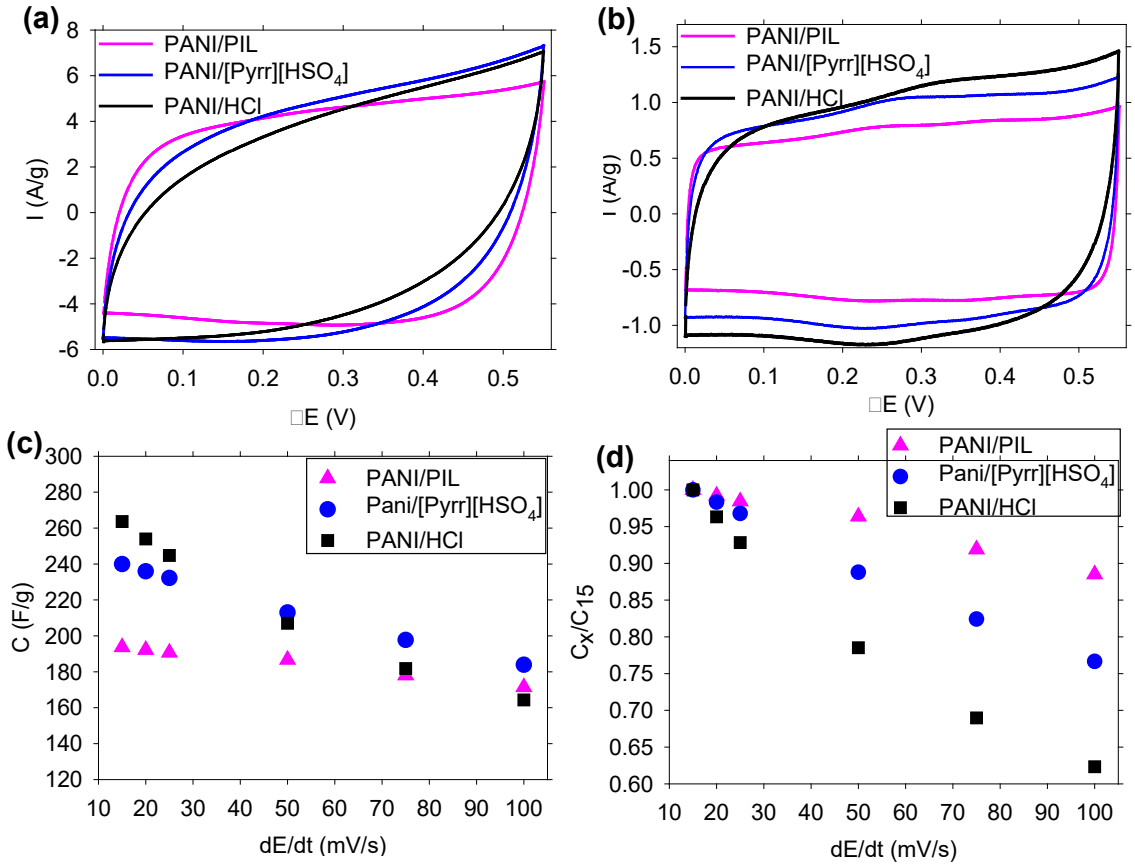

Fig. 7. (**a**) and (**b**) CV curves at a scan rate of 100 and 15 mV/s , respectively, recorded using a two-electrode configuration system, (**c**) specific capacitance from CV discharge curves and (d) capacitance retention by the scan rate (where C_x and C_{15} are the specific capacitance at x and 15 mV/s, respectively) in H_2SO_4 (1 mol/L) of PANI/PIL, PANI/[Pyrr][HSO_4] and PANI/HCl

4. Conclusions

Non-substituted imidazolium-based protic ionic liquid (i.e. [Imi][HSO_4]) was used as a polymerization medium for PANI. The morphology, physicochemical properties, and electrochemical performances of PANI (*i.e.* PANI/PIL) were compared with those of the conventional PANI (*i.e.* PANI/HCl). [Imi][HSO_4] acted as a soft template agent and induced a fibrillar morphology of PANI/PIL instead of agglomerated particles of PANI/HCl. The electrical conductivity of PANI/PIL (21.8 S/cm) was much higher than that of PANI/HCl (3 S/cm). PANI/PIL as electrode material was less resistive than PANI/HCl and had an effective specific capacitance with the scan rate. Compared to substituted ionic liquids based on imidazolium, the non-substituted imidazolium-based protic ionic liquid can be an excellent alternative as it offers many advantages: simple synthesis, high acidity but non-corrosively, inexpensive starting materials, and the synthesis of PANI with controlled properties. At the present stage, it is concluded that [Imi][HSO_4] as a polymerization medium of PANI improves its electrochemical performances and related properties. However, more synthesis conditions (temperature, time, stirring, PIL/water weight ratio, and others) have to be investigated to optimize the PANI/PIL material and further increase its performance.

Author Contributions: conceptualization, M.T and F.T-V.; methodology, F.A-Z.; software, F. A-Z, F.G.; validation, F. T-V., F.G.; formal analysis, F. A-Z, M. A and B.S.; investigation, B.S and F.G.; resources, F. T-V.; data curation, F. A-Z, F.G and B.S; writing—original draft preparation, F. A-Z., B.S, F.G, M.A and KC; writing—review and editing F.T-V and M.T; visualization, F.G and B.S.; supervision, F. T-V".

Funding: "This research was funded by RESCOLL-French Research Company and the Lebanese University".

Acknowledgments: We would like to acknowledge Dr. Martial DEGBIA from IKAMBA Organics laboratory for the helpful discussion. We also wish to thank Dr. Mathieu OYHARCABAL from RESCOLL society for conductivity measurements and Dr. Johan JACQUEMIN for the calculation of the ions surface polarization.

Conflicts of Interest: The authors declare no conflict of interest.

References

1. Veerasubramani, G.K.; Krishnamoorthy, K.; Radhakrishnan, S.; Kim, N.-J.; Kim, S.J. In-situ chemical oxidative polymerization of aniline monomer in the presence of cobalt molybdate for supercapacitor applications. *J Ind Eng Chem* **2016**, *36*: 163–8.
2. Chellachamy, A.A.; Sawant, S.N. Brine solution-driven synthesis of porous polyaniline for supercapacitor electrode application. *Polymer*. **2016**, *87*: 129–37.
3. Bhandari, S.; Khastgir, D. Template-free solid state synthesis of ultra-long hairy polyaniline nanowire supercapacitor. *Mater Lett*. **2014**, *135*: 202–5.
4. Gholivand, M.B.; Heydari, H.; Abdolmaleki, A.; Hosseini, H. Nanostructured CuO/PANI composite as supercapacitor electrode material. *Mater Sci Semicond Process*. **2015**, *30*:157–61.
5. Wang, X.; Liu, D.; Deng, J.; Duan, X.; Guo, J.; Liu, P. Improving cyclic stability of polyaniline by thermal crosslinking as electrode material for supercapacitors. *RSC Adv*. **2015**, *5*:78545–52.
6. Khdary, N.H.; Abdesalam, M.E.; El Enany, G. Mesoporous Polyaniline Films for High Performance Supercapacitors. *J Electrochem Soc*. **2014**, *161*:G63–G8.
7. Wang, G.; Zhang, L.; Zhang, J. A review of electrode materials for electrochemical supercapacitors. *Chem Soc Rev*. **2012**, *41*:797–828.
8. Ramya, R.; Sivasubramanian, R.; Sangaranarayanan, M.V. Conducting polymers-based electrochemical supercapacitors-Progress and prospects. *Electrochim Acta*. **2013**, *101*:109–29.
9. Snook, G.A.; Kao, P.; Best, A.S. Conducting-polymer-based supercapacitor devices and electrodes. *J Power Sources*. **2011**, *196*:1–12.
10. Bhadra, S.; Khastgir, D.; Singha, N.K.; Lee, J.H. Progress in preparation, processing and applications of polyaniline. *Prog Polym Sci*. **2009**, *34*: 783–810.
11. Pauliukaite, R.; Brett, C.M.A.; Monkman, A.P. Polyaniline fibres as electrodes.: Electrochemical characterisation in acid solutions. *Electrochim Acta*. **2004**, *50*:159–67.
12. Al-Zohbi, F. Research Progress on Polyanilie-ionic liquids for Long Cycle-Stable Supercapacitors with High Capacitance. *Appl Funct Mater*. **2022**, 2:51–66.
13. Huang, W.S.; Humphrey, B.D.; MacDiarmid, A.G. Polyaniline, a novel conducting polymer. Morphology and chemistry of its oxidation and reduction in aqueous electrolytes. *J Chem Soc, Faraday Trans 1*. **1986**, *82*: 2385–400.
14. Chaudhari, S.; Sharma, Y.; Archana, P.S.; Jose, R.; Ramakrishna, S.; Mhaisalkar, S.; et al. Electrospun polyaniline nanofibers web electrodes for supercapacitors. *J Appl Polym Sci*. **2013**, *129*:1660–8.
15. Prakash, R. Electrochemistry of polyaniline: Study of the pH effect and electrochromism. *J Appl Polym Sci.* **2002**, *83*: 378–85.
16. Jeon, J.-W.; Ma, Y.; Mike, J.F.; Shao, L.; Balbuena, P.B.; Lutkenhaus, J.L. Oxidatively stable polyaniline:polyacid electrodes for electrochemical energy storage. *Phys Chem Chem Phys*. **2013**, *15*:9654–62.
17. Wang, K.; Huang, J.; Wei, Z. Conducting Polyaniline Nanowire Arrays for High Performance Supercapacitors. *J Phys Chem C*. **2010**, *114*: 8062–7.
18. Gao H, Jiang T, Han B, Wang Y, Du J, Liu Z, et al. Aqueous/ionic liquid interfacial polymerization for preparing polyaniline nanoparticles. *Polymer*. **2004**, *45*:3017–9.
19. Li, X.; Liu, Y.; Guo, W.; Chen, J.; He, W.; Peng, F. Synthesis of spherical PANI particles via chemical polymerization in ionic liquid for high-performance supercapacitors. *Electrochim Acta* **2014**, *135*: 550–7.
20. Pahovnik, D.; Žagar, E.; Vohlidal, J.; Žigon, M. Ionic liquid-induced formation of polyaniline nanostructures during the chemical polymerization of aniline in an acidic aqueous medium. *Synth Met*. **2010**, *160*:1761–6.
21. Pahovnik, D.; Žagar, E.; Kogej, K.; Vohlidal, J.; Žigon, M. Polyaniline nanostructures prepared in acidic aqueous solutions of ionic liquids acting as soft templates. *Eur Polym J*. **2013**, *49*, 1381–90.
22. Krishna, A.; Laslau, C.; Waterhouse, G.I.N.; Zujovic, Z.D.; Travas-Sejdic, J. Effect of ionic liquid on polyaniline chemically synthesised under falling-pH conditions. *Chemical Papers*. **2013**, *67*: 995–1001.
23. Yang, D.; Fadeev, A.G.; Adams, P.N.; Mattes, B.R. GPC characterization of emeraldine base in NMP containing ionic liquids. *Synth Met*. **2007**, *157*: 988–96.
24. Stejskal, J.; Dybal, J.; Trchova, M. The material combining conducting polymer and ionic liquid: Hydrogen bonding interactions between polyaniline and imidazolium salt. *Synth Met*. **2014**, *197*:168–74.
25. Lu, W.; Fadeev, A.G.; Qi, B.; Smela, E.; Mattes, B.R.; Ding, J.; et al. Use of ionic liquids for pi-conjugated polymer electrochemical devices. *Science*. **2002**, *297*: 983–7.
26. Bicak, N.; Senkal, B.F.; Sezer, E. Preparation of organo-soluble polyanilines in ionic liquid. *Synth Met*. **2005**, *155*:105–9.
27. Al-Zohbi, F.; Jacquemin, J.; Ghamouss, F.; Schmaltz, B.; Abarbri, M.; Cherry, K.; et al. Impact of the aqueous pyrrolidinium hydrogen sulfate electrolyte formulation on transport properties and electrochemical performances for polyaniline-based supercapacitor. *J Power Sources*. **2019**, *431*: 162–9.

28. Snook. G.A.; Greaves. T.L.; Best, A.S. A comparative study of the electrodeposition of polyaniline from a protic ionic liquid, an aprotic ionic liquid and neutral aqueous solution using anilinium nitrate. *J Mater Chem*. **2011**, *21*: 7622–9.
29. Li, S.; Yang, C.; Sarwar, S.; Nautiyal, A.; Zhang, P.; Du, H.; et al. Facile synthesis of nanostructured polyaniline in ionic liquids for high solubility and enhanced electrochemical properties. *Adv Compos Hybrid Mater*. **2019** June 01;*2*: 279–88.
30. Anouti, M.; Porion, P.; Brigouleix, C.; Galiano, H.; Lemordant, D. Transport properties in two pyrrolidinium-based protic ionic liquids as determined by conductivity, viscosity and NMR self-diffusion measurements. *Fluid Phase Equilib*. **2010 2008**; *299*: 229–37.
31. Al-Zohbi, F.; Ghamouss, F.; Schmaltz, B.; Abarbri, M.; Zaghrioui, M.; Tran-Van, F. Enhanced Storage Performance of PANI and PANI/Graphene Composites Synthesized in Protic Ionic Liquids. *Materials*. **2021**, *14*: 4275–91.
32. Ahlrichs, R.; Bär, M.; Häser, M.; Horn, H.; Kölmel, C. Electronic structure calculations on workstation computers: The program system turbomole. *Chem Phys Lett*. **1989**, *162*: 165–9.
33. Coadou, E.; Goodrich, P.; Neale, A.R.; Timperman, L.; Hardacre, C.; Jacquemin, J.; et al. Synthesis and Thermophysical Properties of Ether-Functionalized Sulfonium Ionic Liquids as Potential Electrolytes for Electrochemical Applications. *Chem Phys Chem*. **2016**, *17*: 3992–4002.
34. Weigend, F.; Häser, M. RI-MP2: first derivatives and global consistency. *Theor Chem Acc*. **1997**, *97*:331–40.
35. Weigend, F; Häser, M.; Patzelt, H.; Ahlrichs, R. RI-MP2: optimized auxiliary basis sets and demonstration of efficiency. *Chem Phys Lett*. **1998**, *294*: 143–52.
36. Becke, A.D. Density-functional exchange-energy approximation with correct asymptotic behavior. *Phys Rev A*. **1988**, *38*:3098–100.
37. Lee, C.; Yang, W.; Parr, R.G. Development of the Colle-Salvetti correlation-energy formula into a functional of the electron density. *Phys Rev B*. **1988**, *37*:785–9.
38. Grimme, S. Semiempirical GGA-type density functional constructed with a long-range dispersion correction. *J Comput Chem*. **2006**, *27*: 1787–99.
39. Stejskal, J.; Prokeš, J.; Trchová, M. Reprotonation of polyaniline: A route to various conducting polymer materials. *React Funct Polym*. **2008**, *68*: 1355–61.
40. Trchová, M.; Šeděnková, I.; Tobolková, E.; Stejskal, J. FTIR spectroscopic and conductivity study of the thermal degradation of polyaniline films. *Polym Degrad Stab* **2004**, *86*: 179–85.
41. Stejskal, J.; Sapurina, I.; Trchová¡, M.; Prokeš, J.; Křivka, I.; Tobolková, E. Solid-State Protonation and Electrical Conductivity of Polyaniline. Macromolecules. **1998**, *31*: 2218–22.
42. Kulkarni, M.V.; Viswanath, A.K.; Aiyer, R.C.; Khanna, P.K. Synthesis, characterization, and morphology of p-toluene sulfonic acid-doped polyaniline: A material for humidity sensing application. *J Polym Sci, Part B: Polym Phys*. **2005**, *43*: 2161–9.
43. Jayamurugan, P.; Mariappan, R.; Ponnuswamy, V.; Manikandan, H.; Asokan, S.; Saravanan, S. High-PL efficiency of polyaniline using various dopants. *Optik* **2011**, *122*: 2083–5.
44. Li, J.; Tang, X.; Li, H.; Yan, Y.; Zhang, Q. Synthesis and thermoelectric properties of hydrochloric acid-doped polyaniline. *Synth Met.* **2010**, *160*: 1153–8.
45. Quillard, S.; Louam, G.; Buisson, J.P.; Boyer, M.; Lapkowski, M.; Pron, A.; Lefrant, S. Vibrational spectroscopic studies of the isotope effects in polyaniline. *Synth Met*. **1997**, *84*: 805–6.
46. Zhu, H.; Peng, S.; Jiang, W. Electrochemical properties of PANI as single electrode of electrochemical capacitors in acid electrolytes. *Sci World J*. **2013**, *2013*: 940153–62.
47. Zhao, Y.; Wei, H.; Arowo, M.; Yan, X.; Wu, W.; Chen, J.; et al. Electrochemical energy storage by polyaniline nanofibers: high gravity assisted oxidative polymerization vs. rapid mixing chemical oxidative polymerization. *Phys Chem Chem Phys*. **2015**, *17*: 1498–502.
48. Kuang, H.; Cao, Q.; Wang, X.; Jing, B.; Wang, Q.; Zhou, L. Influence of the reaction temperature on polyaniline morphology and evaluation of their performance as supercapacitor electrode. *J Appl Polym Sci*. **2013**, *130*: 3753–8.
49. Grover, S.; Goel, S.; Marichi, R.B.; Sahu, V.; Singh, G.; Sharma, R.K. Polyaniline All Solid-State Pseudocapacitor: Role of Morphological Variations in Performance Evolution. *Electrochim Acta*. **2016**, *196*: 131–9.
50. Kulkarni, M.V.; Viswanath, A.K. Comparative studies of chemically synthesized polyaniline and poly(o-toluidine) doped with p-toluene sulphonic acid. *Eur Polym J*. **2004**, *40*:379–84.
51. Saranya, S.; Selvan, R.K.; Priyadharsini, N. Synthesis and characterization of polyaniline/MnWO4 nanocomposites as electrodes for pseudocapacitors. *Appl Surf Sci*. **2012**, *258*: 4881–7.
52. Gomes, E.C.; Oliveira, M.A.S. Chemical polymerization of aniline in hydrochloric acid (HCl) and formic acid (HCOOH) media. Differences between the two synthesized polyanilines. *Am J Polym Sci*. **2012**, *2*: 5–13.
53. Sapurina, I.Y.; Stejskal, J. Oxidation of aniline with strong and weak oxidants. *Russ J Gen Chem*. **2012**, *82*: 256–75.
54. Cao, Y.; Andreatta, A.; Heeger, A.J.; Smith, P. Influence of chemical polymerization conditions on the properties of polyaniline. *Polymer*. **1989**, *30*: 2305–11.

55. Stejskal, J.; Sapurina, I.; Trchová, M. Polyaniline nanostructures and the role of aniline oligomers in their formation. *Prog Polym Sci*. **2010**, *35*: 1420–81.
56. Sapurina, I.; Stejskal, J. The mechanism of the oxidative polymerization of aniline and the formation of supramolecular polyaniline structures. *Polym Int* **2008**, *57*, 1295–325.
57. Bubnova, O.; Khan, Z.U.; Wang, H.; Braun, S.; Evans, D.R.; Fabretto, M.; et al. Semi-metallic polymers. *Nat Mater*. **2014**, *13*:190-4.
58. Lee, K.; Cho, S.; Heum Park, S.; Heeger, A.J.; Lee, C.-W.; Lee, S.-H. Metallic transport in polyaniline. *Nature*. **2006**, *441*: 65–8.
59. Yue, J.; Gordon, G.; Epstein, A.J. Comparison of different synthetic routes for sulphonation of polyaniline. *Polymer*. **1992**, *33*: 4410–8.
60. Stejskal, J.; Gilbert, RG. Polyaniline. Preparation of a conducting polymer (IUPAC technical report). *Pure Appl Chem*. **2002**, *74*: 857–67.
61. Stejskal, J.; Hlavata, D.; Holler, P.; Trchova, M.; Prokes, J.; Sapurina, I. Polyaniline prepared in the presence of various acids: A conductivity study. *Polym Int*. **2004**, *53*: 294–300.
62. Feng, W.; Zhang, Q.; Li, Y., Feng, Y. Preparation of sulfonated graphene/polyaniline composites in neutral solution for high-performance supercapacitors. *J Solid State Electrochem*. **2014**, 18: 1127–35.
63. Basnayaka, P.A.; Ram, M.K.; Stefanakos, E.K.; Kumar, A. Supercapacitors based on graphene-polyaniline derivative nanocomposite electrode materials. *Electrochim Acta*. **2013**, *92*: 376–82.
64. Cui, Q.; Mi, H.; Qiu, J.; Yu, C.; Zhao, Z. Interconnected polyaniline clusters constructed from nanowires: Confined polymerization and electrochemical properties. *J Mater Res*. **2014**, *29*: 2408–15.
65. Meng, Q.; Cai, K.; Chen, Y.; Chen, L. Research progress on conducting polymer based supercapacitor electrode materials. *Nano Energy*. **2017**, *36*: 268–85.